Comparison of Several Finite Difference Methods for Magnetohydrodynamics in 1D and 2D

Petr Havlík[1] and Richard Liska[1]

Faculty of Nucl. Sci. and Phys. Engrg., Czech Technical University in Prague, Břehová 7, 115 19 - Praha 1, Czech Republic xhavlik@fermi.fjfi.cvut.cz , liska@siduri.fjfi.cvut.cz

Summary. The comparison of several finite difference methods for ideal magneto-hydrodynamics (MHD) is presented. Compared finite difference methods include composite schemes, central scheme, WENO, component wise CWENO and public freely available packages Nirvana and Flash. 1D Cartesian tests concern smooth, Brio-Wu and intermediate shock formation problems. From 2D Cartesian tests we shortly present Orszag-Tang vortex problem and shock-cloud interaction problem. As we are interested in the generalization of schemes from Cartesian to cylindrical $r-z$ geometry, we include also generalization of composite and CWENO schemes to cylindrical geometry with their application to 2D conical z-pinch problem.

1 Introduction

For simplicity we use the system of ideal magneto-hydrodynamics (MHD) equations in dimensionless units (with magnetic permeability $\mu = 1$)

$$\frac{\partial \varrho}{\partial t} + \nabla \cdot (\varrho \mathbf{v}) = 0, \tag{1}$$

$$\frac{\partial (\varrho \mathbf{v})}{\partial t} + \nabla \cdot \left(\varrho \mathbf{v}\mathbf{v}^{\mathrm{T}} + \mathrm{P}^{\star}\mathrm{I}^{3\times 3} - \mathbf{B}\mathbf{B}^{\mathrm{T}} \right) = 0, \tag{2}$$

$$\frac{\partial \mathbf{B}}{\partial t} + \nabla \cdot (\mathbf{v}\mathbf{B}^{\mathrm{T}} - \mathbf{B}\mathbf{v}^{\mathrm{T}}) = 0, \tag{3}$$

$$\frac{\partial E}{\partial t} + \nabla \cdot \left[\mathbf{v} \left(\mathrm{E} + \mathrm{P}^{\star} \right) - \mathbf{B}(\mathbf{v} \cdot \mathbf{B}) \right] = 0, \tag{4}$$

where ϱ is mass density, $\mathbf{v}$ velocity, $\mathbf{B}$ magnetic induction, E total energy and $P^{\star}$ is the sum of hydrodynamic and magnetic pressures $P^{\star} = p + \mathbf{B}^2/2$. Thermodynamical pressure p can be computed from equation of state for ideal gas $p = (\gamma - 1)\left[E - \varrho \mathbf{v}^2/2 - \mathbf{B}^2/2\right]$, where γ is ideal gas constant (ratio of specific heats). The symbol $\mathrm{I}^{3\times 3}$ denotes 3×3 unit matrix and $^{\mathrm{T}}$ transposition. The MHD system (1)–(4) is coupled with constraint

$$\nabla \cdot \mathbf{B} = 0 \tag{5}$$

following directly from Maxwell equations. Using the equation (3) one can verify, that the divergence of solenoidal magnetic field doesn't change in time, i.e. if the condition (5) is satisfied at initial time, it remains valid at any time later. Generally, this property does not hold for a numerical solutions of the system and special techniques have to be used for keeping numerical magnetic field solenoidal.

2 Cartesian geometry

We first shortly describe numerical methods which have been used for comparisons and then present their performance on several 1D and 2D tests in Cartesian geometry. The numerical methods include composite, central, WENO and component wise CWENO finite difference schemes together with the methods used in Nirvana (version 3, `http://nirvana-code.aip.de`) and Flash (version 2.5, `http://flash.uchicago.edu`) free available packages. All methods are of finite difference type and all results have been computed on rectangular uniform mesh. *Composite* scheme [9] performs one Lax-Friendrichs (LF) step after $n-1$ Lax-Wendroff (LW) steps and is denoted as LWLFn. The diffusive LF step serves as a consistent filter removing dispersive LW oscillations appearing behind shock waves. The LW scheme itself is second order accurate, while the LF and LWLFn ones only first. *Central* scheme (source code published in [2]) on the staggered grid uses limited piecewise polynomial reconstruction from cell averages. It requires neither Riemann solver nor eigen-decomposition and also avoids dimensional splitting. *WENO* scheme [8] uses convex weighted combination of essentially non-oscillatory schemes on several stencils for space discretization and Runge-Kutta (RK) methods for time integrating. It is fifth order accurate in space and we denote it as WENO3 in case of RK3 (TVD) time integration method and WENO5 in case of RK4 (non-TVD) method. WENO requires local eigenvector decomposition ([10]) which classifies it to be the slowest scheme from our choice. Avoiding eigen-decomposition and applying WENO procedure directly to the conserved quantities we obtain *CWENO* (Component-wise WENO) scheme. After each time step of the above finite difference scheme the magnetic field is corrected to numerically satisfy the solenoidal condition (5) by the constrained transport method [5, 11]. Flash [6] package uses MUSCL-type limited gradient reconstruction method. Nirvana [12] employs second order semi-discrete Godunov-type central method.

2.1 Smooth periodic problem in 1D

The first 1D problem originates in [7] for Euler equations however it provides an exact solution (periodic in ρ and constant in $\mathbf{v}, \mathbf{B}, p$) for the MHD system

as well. We employ the particular exact solution $\varrho(x,t) = 1 + 0.2\sin(\pi(x - t))$, $v^x(x,t) = 1$, $B^y(x,t) = 1$, $p(x,t) = 1$ which we treat on interval $x \in [0,1]$ till final time $t = 1$ with periodic boundary conditions and $\gamma = 1.4$. Table 1 shows for all numerical methods absolute L_1 errors of density on the grid with 1600 cells (which we denote by $L_1(\varrho, 1600)$) together with the numerical order of accuracy (NOA) given by $\log_2(L_1(\varrho, 800)/L_1(\varrho, 1600))$. As expected:

Table 1. Convergence for smooth periodic problem – $L_1(\varrho, 1600)$ errors and the numerical order of accuracy (NOA) $\log_2(L_1(\varrho, 800)/L_1(\varrho, 1600))$.

scheme	LWLF12	LW	Central	CWENO5	WENO3	WENO5	Flash	Nirvana3
$L_1(\varrho, 1600)$	2.5e-04	5.35e-07	1.01e-06	8.60e-14	1.21e-12	2.05e-14	2.51e-07	9.08e-07
NOA	1.0	2.0	2.4	5.0	3.1	5.0	2.1	2.1

the composite scheme is first order accurate; LW, central, Flash and Nirvana are second order; WENO3 is third order; WENO5 and CWENO5 are fifth order.

2.2 Brio-Wu problem in 1D

The Brio-Wu Riemann problem is classical MHD test problem [3] used in almost all papers numerically treating MHD equations. Here we present only similar results as for previous periodic problem. Table 2 shows $L_1(\varrho, 1600)$ deviations of numerical solution (on mesh with 1600 cells) for density from a reference solution. As the reference solution we use Flash solution with 6400 cells. NOA $\log_2(L_1(\varrho, 800)/L_1(\varrho, 1600))$ is presented in Table 2 too. As expected, all the numerical methods are first order accurate for this problem involving discontinuous waves.

Table 2. Convergence for Brio-Wu test problem – $L_1(\varrho, 1600)$ deviations from Flash solution using 6400 cells and the NOA $\log_2(L_1(\varrho, 800)/L_1(\varrho, 1600))$.

scheme	LWLF12	Central	CWENO3	CWENO5	WENO3	WENO5	Flash	Nirvana3
$L_1(\varrho, 1600)$	2.6e-03	2.1e-03	1.4e-03	1.4e-03	1.0e-03	1.0e-03	6.2e-04	1.5e-03
NOA	0.7	1.0	1.0	1.0	1.0	1.0	1.2	1.0

2.3 Intermediate shock formation in 1D

This test problem, originating in [8], starts from smooth initial conditions from which after some time shocks develop. Initially, $B^y(x) = \sin(2\pi x)/2$ for $x \in [0,1]$ and all other conservative quantities are computed with using generalized Riemann invariants. All quantities are normalized to $\varrho = 1$,

$\mathbf{v} = (0,0,0)^T$, $B^x = 1$, $B^z = 0$ and $p = 1$ at points where $B^y = 0$. Periodic boundary conditions are applied. Table 3 presents $L_1(B^y, 1600)$ deviations of B^y numerical solutions with 1600 cells from the reference WENO5 solution using 6400 cells together with the NOA $\log_2(L_1(\varrho, 800)/L_1(\varrho, 1600))$ at three different times. At time $t = 0.25$ the solution is still smooth (see Fig. 1(a)) and the schemes have the NOA close to that one for smooth test presented in Table 1. In Fig. 1(a) the local deviation $|u_{num}(x) - u_{ref}(x)|$ of the numerical solution from the reference one is continuous and the cumulative deviation $\int_0^x |u_{num}(x') - u_{ref}(x')|dx'$ is smooth function of x showing that the L_1 deviation is distributed over the whole domain $x \in [0,1]$. At time $t = 0.6$ two shocks are already formed around $x = 0.13$ and 0.63 (see Fig. 1(b)) and the NOA decreases rapidly towards one when L_1 deviations are evaluated on the whole computational domain $x \in [0,1]$, while keeping high values when L_1 deviations are evaluated on $x \in [0.2, 0.4]$ where B^y still has smooth profile. In Fig. 1(b) the local deviation $|u_{num}(x) - u_{ref}(x)|$ is close to delta function at two shocks and the cumulative deviation $\int_0^x |u_{num}(x') - u_{ref}(x')|dx'$ has jumps at two shocks showing that most L_1 deviation is concentrated around the shocks. At time $t = 1.0$ the NOA is low even on sub-domain $x \in [0.2, 0.4]$ where B^y is smooth, however the shock, which is now at $x = 0.5$ has already passed through this sub-domain (see Fig. 1(c)).

Table 3. Convergence for intermediate shock formation problem at three times $t = 0.25, 0.6, 1$ – $L_1(B^y, 1600)$ deviations (on $x \in [0,1]$) from WENO5 solution using 6400 cells and the NOA $\log_2(L_1(\varrho, 800)/L_1(\varrho, 1600))$ computed from deviations on $x \in [0,1]$ and on $x \in [0.2, 0.4]$.

scheme	LWLF12	Central	CWENO3	CWENO5	WENO3	WENO5	Flash
$t = 0.25, L_1(B^y, 1600)$	9.3e-05	2.8e-06	1.5e-10	8.1e-12	1.5e-10	9.7e-12	7.8e-07
NOA on $x \in [0,1]$	1.0	2.3	3.1	5.1	3.1	5.1	2.1
$t = 0.6, L_1(B^y, 1600)$	7.4e-04	4.4e-04	2.3e-04	2.3e-04	2.5e-04	2.5e-04	1.8e-04
NOA on $x \in [0,1]$	1.1	1.2	1.2	1.2	1.2	1.2	1.3
NOA on $[0.2, 0.4]$	1.0	2.4	4.2	4.3	4.9	5.0	1.9
$t = 1, L_1(B^y, 1600)$	1.0e-03	7.2e-04	6.9e-04	6.9e-04	3.5e-04	3.5e-04	1.9e-04
NOA on $x \in [0,1]$	0.9	1.0	0.6	0.6	1.1	1.1	1.1
NOA on $[0.2, 0.4]$	1.0	1.2	1.4	1.4	1.5	1.8	1.5

2.4 Orszag-Tang vortex problem in 2D

The Orszag-Tang vortex problem is defined on a square $(x, z) \in [0, 2\pi] \times [0, 2\pi]$ with initial conditions $\varrho = \gamma^2, \mathbf{v} = (-\sin z, 0, \sin x)^T, \mathbf{B} = (-\sin z, 0, \sin(2x))^T$, $p = \gamma$ with $\gamma = 5/3$. Periodic boundary condition are applied in both directions. Fig. 2(a) presents density contours at time $t = 3$ computed by Flash on the mesh with 400×400 cells. 1D cuts along line $z = \pi$ in density are shown

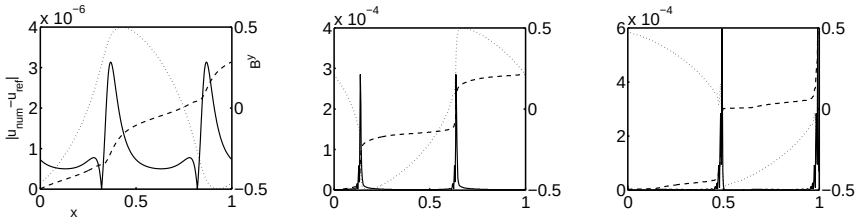

(a)$t = 0.25$ (b) $t = 0.6$ (c) $t = 1$

Fig. 1. Solution $B^y(x)$ by dotted line, local deviation $|u_{num}(x) - u_{ref}(x)|$ (of numerical solution from reference one) by solid line and cumulative deviation $\int_0^x |u_{num}(x') - u_{ref}(x')|dx'$ by dashed line for composite LWLF12 scheme (other schemes produce similar plots) with 400 cells at three times $t = 0.25, 0.6, 1$. Cumulative deviation at point $x = 1$ equals 9.7e-7 for $t = 0.25$, 6.8e-6 for $t = 0.6$ and 1.1e-5 for $t = 0.1$.

for all schemes in Fig. 2(b)-(c), where the differences between the schemes can be seen. Results are for clarity split into 2 Figs. with identical axes and one reference (Flash) solution. Results can be compared with [2, 4, 8, 12].

2.5 Shock cloud interaction problem in 2D

The initial conditions for the shock cloud interaction problem [4, 11, 12] consist of two states in $(x, z) \in [-1/2, 1/2] \times [-1/2, 1/2]$ separated by shock discontinuity along line $x = 0.1$. The left state is defined by values $\varrho = 3.86859$, $\mathbf{v} = (0, 0, 0)^T$, $\mathbf{B} = (0, 2.1826182, -2.1826182)^T$, $p = 167.345$ while the right state is defined by values $\varrho = 1$, $\mathbf{v} = (-11.2536, 0, 0)^T$, $\mathbf{B} = (0, 0.56418958, 0.56418958)^T$, $p = 1$. At point $(0.3, 0)$ a spherical density clump with radius 0.15 and constant density $\varrho = 10.0$ and pressure $p = 1$ is located. On contour map of pressure in Fig. 2 (d) we show result of Nirvana scheme computed on grid with 400×400 cells at time $t = 0.06$. Composite scheme has remarkably lower sharpness of shock wave, while Nirvana and Flash have both much better shock wave resolution, however the profile of density clump deformed by passing shock wave differs. The 2D profile from CWENO is closer to Nirvana. WENO scheme failed for this test during computation. 1D cuts of pressure in Fig. 2(e)-(f) along the line $z = 0$ show profiles of all methods. More differences can be seen in composite scheme results, which profiles are in some regions shifted, e.g. transmitted shock wave behind the clump is slower.

3 Cylindrical geometry

In Cartesian geometry, there are no source terms and the MHD system (1)–(4) is in conservative form. On the other hand, in cylindrical geometry the

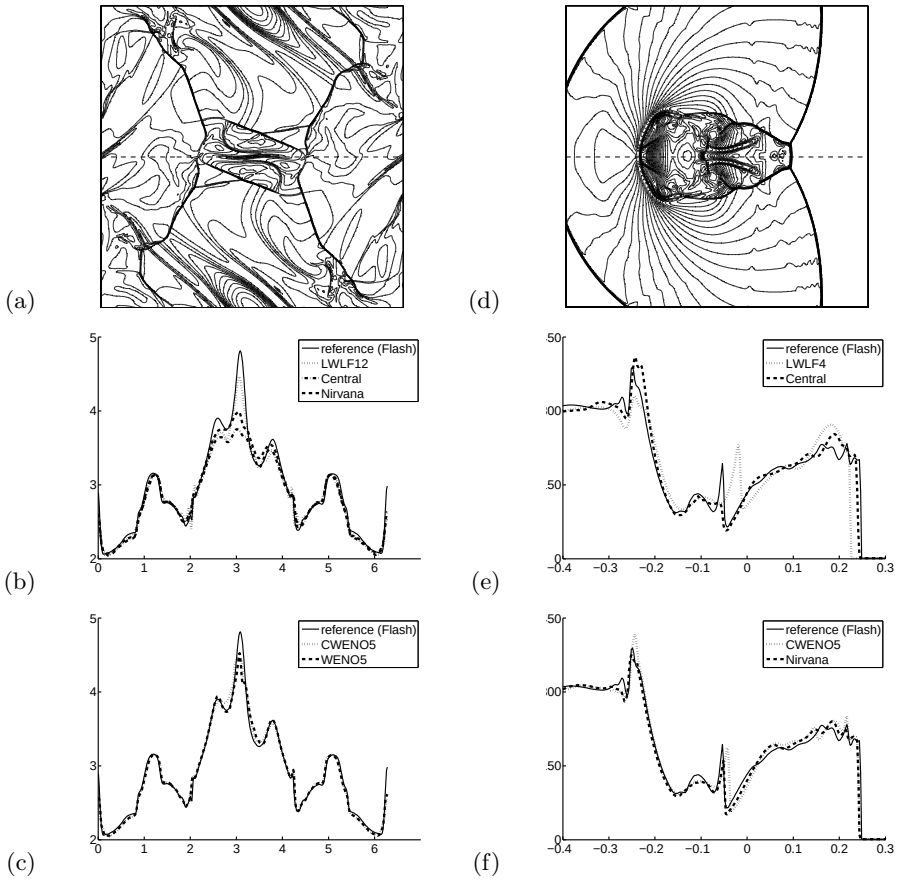

Fig. 2. Density contours for Orszag-Tang vortex by Flash (a); 1D slices in density along line $z = \pi$ for Orszag-Tang vortex (b), (c); pressure contours for shock-cloud interaction problem by Nirvana (d); 1D slices in pressure along line $z = 0$ for shock-cloud interaction problem (e), (f).

divergence has the form $\nabla_{cyl} \equiv (1/r + \partial/\partial r, 1/r\,\partial/\partial\varphi, \partial/\partial z)$ which introduces geometrical source terms and the system is not conservative. Most of the geometric source terms can be included into the fluxes by multiplying the MHD system (except the equation for B^{φ}) by radius r. Then the source terms remain only in two equations for momentum conservation in r and φ directions. We have available only two methods - composite and CWENO schemes in 2D cylindrical $r - z$ geometry. Both LW and LF schemes in the composite use simple averaging to get the source terms on staggered mesh, just LW corrector uses sources from previous time step. CWENO scheme in cylindrical geometry has been developed as extension from Cartesian geometry. It employs the same weighted approximation procedure as for fluxes evaluation to

get the source terms at the edges midpoints. The sources are averaged from the edges midpoints to get the source term inside the cell. Flash [6] supports MHD only in Cartesian geometry, we were quite surprised that with MHD setup in cylindrical geometry Flash happily computes in Cartesian geometry without any warning. Nirvana [12] does not include cylindrical MHD.

3.1 Conical z-pinch in 2D

This test coming from [1] simulates compression of conical z-pinch by magnetic field. The problem is solved on rectangular area $(r, z) \in [0, 1.3] \times [0, 1]$ with initial conditions given by values $\varrho = 1$, $\mathbf{B} = (0, 0, 0)^T$ for $r \leq 1 + 0.3z$ holds and by values $\varrho = 10^{-4}$, $\mathbf{B} = (0, \sqrt{2}/r, 0)^T$ elsewhere. Velocity and pressure are same in the whole area $\mathbf{v} = (0, 0, 0)^T$ and $p = 10^{-4}$. Free boundary conditions on top at $z = 1$, bottom at $z = 0$ and free on right at $r = 1.3$ except Dirichlet boundary conditions $B^\varphi = \sqrt{2}/r$ for B^φ keeping the tangential magnetic induction. Fig. 3 presents pressure contours and velocity fields by arrows obtained for this problem by composite (a) and CWENO (b) cylindrical schemes at time $t = 0.63$ on grid with 400×400 cells. Composite scheme is not able to resolve instabilities, seen in CWENO result. Similar instabilities appear also in [1].

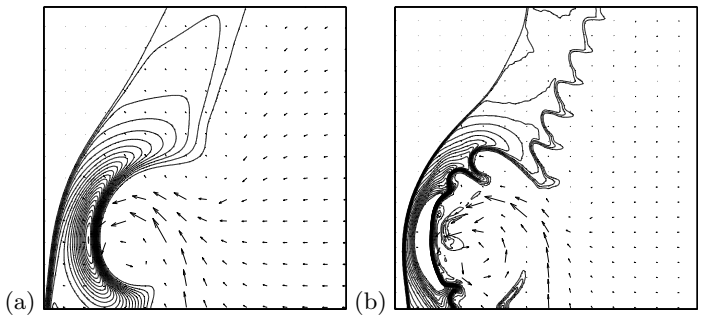

Fig. 3. B^y contours and velocity field by arrows of LWLF80 (a) and CWENO5 (b) for conical z-pinch in cylindrical geometry.

4 Conclusion

Selected finite difference methods have been applied to a set of 1D and 2D test problems in Cartesian geometry and their numerical results have been compared. The results of composite schemes are the worst between others in the sense of resolution discontinuities. The most precise results in regions of smooth solution are typically obtained by WENO scheme, however it is

very slow due to eigenvector decomposition and it fails in some cases as e.g. for shock cloud interaction problem. In most cases component-wise CWENO scheme produces results very close to WENO, however in some cases, as e.g. for Brio-Wu problem, it produces very mild oscillations in regions of flat solution between the waves. In general it seems that the best results are obtained from Flash code, which is moreover remarkably fast. Nirvana produces also very good results. Composite and CWENO have been generalized to cylindrical $r - z$ geometry.

Acknowledgment: This research has been partly supported by the Czech Ministry of Education project MSM 6840770022, research center LC 528, Czech Technical University project CTU0621814 and the Czech Science Foundation project GACR 202/03/H162. The software Flash used in this work was in part developed by the DOE-supported ASCI / Alliance Center for Astrophysical Thermonuclear Flashes at the University of Chicago.

References

1. Aksenov, A.G.; Gerusov, A.V.: Comparative Analysis of Numerical Methods for 2-Dimensional High Compression MHD Flow Simulation, Plasma Physics Reports **21** (1): 11–19 Jan 1995
2. Balbas, J.; Tadmor, E.; Wu, C.-C.: Non-Oscillatory Central Schemes for One- and Two-Dimensional MHD Equations: I, J. of Comput. Phys. **201** (2004) 261–285
3. Brio, M,; Wu, C.C.: An Upwind Differencing Scheme for the Equations of Ideal Magnetohydrodynamics, J. of Comput. Phys. **75** (1998) 400–422
4. Dai, W.; Woodward, P.R.: A Simple Finite Difference Scheme for Multidimensional Magnetohydrodynamical Equations, J. of Comput. Phys. **142** (1998) 331–369
5. Evans, C.R.; Hawley, J.F.: Simulation of Magnetohydrodynamic Flows – A Constrained Transport Method, The Astrophysical J., 332:659–677, 1988
6. ASC FLASH Center: FLASH user's guide, version 2.3/2.5, University of Chicago, 2003/2005
7. Jiang, G.S.; Shu, C.W.: Efficient Implementation of Weighted ENO Schemes, J. Comp. Phys. **126** (1996) 202–228
8. Jiang, G.-S.; Wu, C.-C.: A High-Order WENO Finite Difference Scheme for the Equations of Ideal Magnetohydrodynamics, J. of Comput. Phys. **150** (1999) 561–594
9. Liska, R.; Wendroff, B.: Composite Schemes for Conservation Laws, SIAM J. Sci. Comput. **35**, no. 6 (1998) 2250–2271
10. Roe, P.L.; Balsara, D.S.: Notes on the Eigensystem of Magnetohydrodynamics, SIAM J. Appl. Math. **56**, no. 1 (1996) 57–61
11. Tóth, G.: The $\nabla \cdot \mathbf{B}$ Constraint in Shock-Capturing Magnetohydrodynamics Codes, J. of Comput. Phys. **161** (2000) 605–652
12. Ziegler, U.: A Central-constrained Transport Scheme for Ideal Magnetohydrodynamics, J. of Comput. Phys. **196** (2004) 393–416